CCR2 recruits an inflammatory macrophage subpopulation critical for angiogenesis in tissue repair

*Sebastian Willenborg,[1] *Tina Lucas,[1] Geert van Loo,[2,3] Johanna A. Knipper,[1] Thomas Krieg,[1,4,5] Ingo Haase,[1] Bent Brachvogel,[4,6] Matthias Hammerschmidt,[4,5,7] Andras Nagy,[8] Napoleone Ferrara,[9] Manolis Pasparakis,[4,5,10] and Sabine A. Eming[1,4,5]

[1]Department of Dermatology, University of Cologne, Cologne, Germany; [2]Department for Molecular Biomedical Research, Vlaams Instituut voor Biotechnologie, Ghent, Belgium; [3]Department of Biomedical Molecular Biology, Ghent University, Ghent, Belgium; [4]Center for Molecular Medicine Cologne, University of Cologne, Cologne, Germany; [5]Cologne Excellence Cluster on Cellular Stress Responses in Aging-Associated Diseases, University of Cologne, Cologne, Germany; [6]Center for Biochemistry, Medical Faculty, University of Cologne, Cologne, Germany; [7]Institute for Developmental Biology, University of Cologne, Cologne, Germany, Belgium; [8]Samuel Lunenfeld Research Institute, Mount Sinai Hospital, Toronto, ON; [9]Genentech Inc, South San Francisco, CA; and [10]Institute for Genetics, University of Cologne, Cologne, Germany

Monocytes/macrophages are critical in orchestrating the tissue-repair response. However, the mechanisms that govern macrophage regenerative activities during the sequential phases of repair are largely unknown. In the present study, we examined the dynamics and functions of diverse monocyte/macrophage phenotypes during the sequential stages of skin repair. By combining the analysis of a new CCR2-eGFP reporter mouse model with conditional mouse mutants defective in myeloid cell–restricted CCR2 signaling or VEGF-A synthesis, we show herein that among the large number of inflammatory CCR2$^+$Ly6C$^+$ macrophages that dominate the early stage of repair, only a small fraction strongly expresses VEGF-A that has nonredundant functions for the induction of vascular sprouts. The switch of macrophage-derived VEGF-A during the early stage of tissue growth toward epidermal-derived VEGF-A during the late stage of tissue maturation was critical to achieving physiologic tissue vascularization and healing progression. The results of the present study provide new mechanistic insights into CCR2-mediated recruitment of blood monocyte subsets into damaged tissue, the dynamics and functional consequences of macrophage plasticity during the sequential repair phases, and the complementary role of macrophage-derived VEGF-A in coordinating effective tissue growth and vascularization in the context of tissue-resident wound cells. Our findings may be relevant for novel monocyte-based therapies to promote tissue vascularization. (*Blood*. 2012;120(3):613-625)

Introduction

Tissue injury induces a dynamic and complex repair program proceeding in sequential phases of tissue growth and differentiation.[1] In postnatal life, recruitment of circulating blood monocytes to the site of tissue damage and their differentiation into tissue macrophages at the wound site are critical to reconstituting tissue integrity.[2,3] During the diverse stages of the healing response, monocytes/macrophages have pleiotropic functions and may provide important targets for novel monocyte-based therapies to stimulate wound healing and/or to interfere with the pathology of tissue repair. However, the mechanisms that mediate monocyte recruitment to damaged tissue and that govern their regenerative activities during the sequential phases of tissue growth and differentiation are poorly understood.

Vascularization is essential for most physiologic and pathologic processes of tissue growth and macrophages have long been recognized as critical regulators of angiogenesis.[4-6] During the early stages of skin wound healing, angiogenesis is fundamental for the effective development of dermal tissue and is a hallmark of an established healing response. In fact, attenuated angiogenesis is the major pathology underlying common impaired healing conditions.[1,7] A mechanistic understanding of macrophage-specific activities in blood vessel growth is just beginning to emerge. Using models of selective and inducible cell depletion, we and others recently reported on functional heterogeneity for monocyte/macrophage subsets in tissue vascularization.[3,4,8-11] Myeloid cell-derived VEGF-A has been shown to play a critical role in blood vessel growth.[12-14] Therefore, selective targeting of monocyte/macrophage subpopulations for proangiogenic therapy may provide an attractive strategy in regenerative processes. However, the dynamics and function of proangiogenic tissue macrophages and how they may control vascular growth in concert with other cellular sources of proangiogenic mediators are not completely understood.

Macrophages are highly plastic cells, and various functional phenotypes have been described, including M1 macrophages (classically activated), which exert proinflammatory activities, and M2 macrophages (alternatively activated), which are involved in the resolution of inflammation.[15] Effective vascularization in particular has been attributed to the M2 phenotype,[4,16] which is often referred to as the "repair macrophage phenotype." However,

Submitted January 18, 2012; accepted April 26, 2012. Prepublished online as *Blood* First Edition paper, May 10, 2012; DOI 10.1182/blood-2012-01-403386.

*S.W. and T.L. contributed equally to this work.

There is an Inside *Blood* commentary on this article in this issue.

The online version of this article contains a data supplement.

The publication costs of this article were defrayed in part by page charge payment. Therefore, and solely to indicate this fact, this article is hereby marked "advertisement" in accordance with 18 USC section 1734.

conclusive evidence as to whether the general concept of M1/M2 polarization is operative at the cutaneous wound site and/or if wound vascularization requires a specific macrophage activation state is still missing.

Blood monocytes are also a heterogeneous population of cells, and there is currently substantial debate about whether specific monocyte populations give rise to specific tissue macrophage phenotypes.[17] To date, 2 functional subsets among murine blood monocytes have been identified: a chemokine-receptor-2$^+$ (CCR2$^+$) and Ly6C$^+$ "inflammatory" subset and a less-characterized, CCR2$^-$Ly6C$^-$ "noninflammatory" subset.[18,19] It is not completely understood whether a peripheral monocyte subset may be preferentially recruited into the lesion in different tissues and whether these cells acquire a specific state of macrophage activation that monitors the repair response and promotes tissue vascularization.

To examine the functional impact of the origin and activation of monocyte/macrophage subsets to skin repair and wound angiogenesis, in the present study, we characterized monocyte/macrophage phenotypes and functions during the diverse phases of the healing response after excision skin injury. Our findings extend mechanistic insight into the dynamics, regulation, and function of monocytes/macrophages during tissue vascularization and regeneration.

Methods

Animals

The generation of the CCR2^{fl}-enhanced green fluorescent protein (CCR2^{fl}-eGFP) mice (C57BL/6 background) will be described elsewhere (G.v.L. and M.P., manuscript in preparation). To generate mice with *CCR2* gene deletion in all cell types (CCR2$^{D/D}$), CCR2$^{fl/fl}$ mice were bred to a Cre-transgenic strain expressing Cre recombinase ubiquitously in the early stages of ontogeny.[20] The progeny carried 1 deleted allele in all cell types (CCR2$^{wt/D}$). To generate CCR2$^{D/D}$ mice, heterozygous CCR2$^{wt/D}$ mice were crossed. CCR2-eGFP reporter mice (CCR2$^{fl/D}$) were generated by crossing CCR2$^{D/D}$ mice with CCR2$^{fl/fl}$ mice; thus, in 1 allele eGFP expression is controlled through the *CCR2* promoter activity independent of Cre recombinase activity, whereas the other allele contains a functional *CCR2* gene. VEGF$^{fl/fl}$LysMCre and VEGF$^{fl/fl}$LysMCreK14Cre mice were on the FVB/N background.[21,22] Cre-mediated recombination was verified by PCR analysis in genomic DNA as described previously.[20-24] Mice were maintained and bred under standard pathogen-free conditions. Eight- to 12-week-old male mice were used for the experiments. All animal experiments were approved by the national animal care committee and the University of Cologne.

Cell culture

Peritoneal cells were seeded in 6-well plates (0.5×10^6 cells/cm^2), and macrophages enriched by plastic adhesion were cultured overnight and stimulated with lipopolysaccharide (1 mg/mL; Sigma-Aldrich) and recombinant IFN-γ (0.1 mg/mL; R&D Systems) or exposed to hypoxia (1% O_2, 5% CO_2 for 8 hours); experiments were performed in DMEM (1% FCS). VEGF-A protein in the cell-culture supernatants was quantified by ELISA (Quantikine Immunoassay; R&D Systems). Angiogenesis real-time PCR Array (RT^2 Profiler PCR Array, PAMM-024; SA Bioscience) was used according to the manufacturer's instructions.

Flow cytometric analysis and cell sorting

Blood leukocytes were isolated from heparinized blood by hypotonic lysis of erythrocytes using ammonium chloride-potassium chloride lysing buffer, followed by ice-cold PBS (1% BSA and 2mM EDTA) washes. Wound cells were isolated by a combination of enzymatic digestion (Liberase Blendzyme; Roche Applied Science) and mechanical disruption (Medimachine System; BD Biosciences). For FACS analysis, Fc receptors were blocked with mouse seroblock FcR (CD16/CD32; AbD Serotec) and cells were stained with FITC- or PE-conjugated anti-F4/80 (AbD Serotec), PE-conjugated anti–Gr-1, PE- or APC-conjugated anti-CD11b (Miltenyi-Biotec), APC-conjugated anti-CD115, APC-Cy7–conjugated anti-Ly6G, FITC-conjugated anti-CD19 and anti-CD3e (eBiosciences), and PE-Cy7–conjugated anti-Ly6C (BD Biosciences). The following isotype controls were used: FITC-conjugated rat IgG2a, PE-conjugated rat IgG2b, APC-conjugated rat IgG2b (eBiosciences), and PE-Cy7–conjugated rat IgM (BD Biosciences). Cells were incubated with Abs for 30 minutes at 4°C and washed 3 times thereafter in washing buffer (1% BSA and 2mM EDTA in PBS). Dead cells were excluded using 7-amino-actinomycin D (BD Biosciences). β-Gal activity was visualized by fluorescein di-β-D-galactopyranoside (FDG; Invitrogen) incubation. To allow FDG uptake, cells were incubated in FDG (2mM) in distilled water (20 seconds). The hypotonic shock was stopped by adding ice-cold PBS (1% BSA and 2mM EDTA), followed by incubation with FDG for 1 hour. Cells were analyzed on a FACSCanto II flow cytometer or sorted on a FACSAria III cell sorter using FACSDiva Version 6.1.1 (BD Biosciences) or FlowJo Version 7.6.4 (TreeStar) software.

Wounding and preparation of wound tissues

Wounding and preparation of wound tissue for histology was performed as described previously.[3] Briefly, mice were anesthetized and 4 full-thickness punch biopsies were created on the back. For histologic analysis, wounds were excised at different times after injury, bisected in the caudocranial direction, and the tissue was either fixed overnight in 4% formaldehyde or embedded in optimal cutting temperature compound (Tissue-Tek).

Real-time PCR analysis

RNA from complete wound tissue was isolated using the Fibrous Tissue Mini Kit and RNA from single-cell suspensions was isolated using the RNeasy Mini or Micro Kits (QIAGEN) according to the manufacturer's instructions. Reverse transcription of isolated RNA was performed using the High Capacity cDNA RT Kit (Applied Biosystems). Primers (Sigma-Aldrich) were generated as outlined in supplemental Figure 2 (available on the *Blood* Web site; see the Supplemental Materials link at the top of the online article). Amplification reactions (triplicates) were set up using PowerSYBR Green PCR Master Mix (Applied Biosystems) and quantitative RT-PCR (qRT-PCR) was validated with the 7300 Real Time PCR system (Applied Biosystems). The comparative method of relative quantification ($2^{-\Delta\Delta Ct}$) was used to calculate the expression level of the target gene normalized to S18 or GAPDH. The amplified PCR fragments were a maximum of 250 bp in length and the annealing temperature was 60°C.

Immunohistochemistry

Immunohistochemical stainings (10-μm cryosections) were performed as described previously.[3] Bound primary Abs (anti-CD31, BD Pharmingen; anti-Desmin, DakoCytomation; and anti–δ-like-4 [anti-Dll4], R&D Systems) were detected by incubation with Alexa Fluor 488– or Alexa Fluor 594–conjugated secondary Abs (Invitrogen), followed by counterstaining with DAPI (Invitrogen). Anti–α-smooth muscle actin (αSMA) staining was performed on paraffin sections (6 μm).[25] Specificity of primary Abs was demonstrated by replacing them with irrelevant isotype-matched Abs.

X-Gal staining

For X-Gal staining, 20-μm cryosections were prepared from VEGF-lacZ wound tissues (fixed in 0.5% glutaraldehyde for 30 minutes at room temperature) and washed 3 times in washing buffer (PBS, 0.02% NP-40,and 0.2mM $MgCl_2$). Sections were incubated in X-Gal staining solution containing 0.5 mg/mL of X-Gal (Fermentas), 10mM $K_3[Fe(CN)_6]$, 10mM $K_4[Fe(CN)_6]$, and 0.2mM $MgCl_2$ for 6 hours at 37°C and counterstained with a nuclear fast red aluminium sulfate solution.

Morphometric analysis

Morphometric analysis was performed on H&E-stained paraffin tissue sections using light microscopy equipped with a KY-F75U digital camera

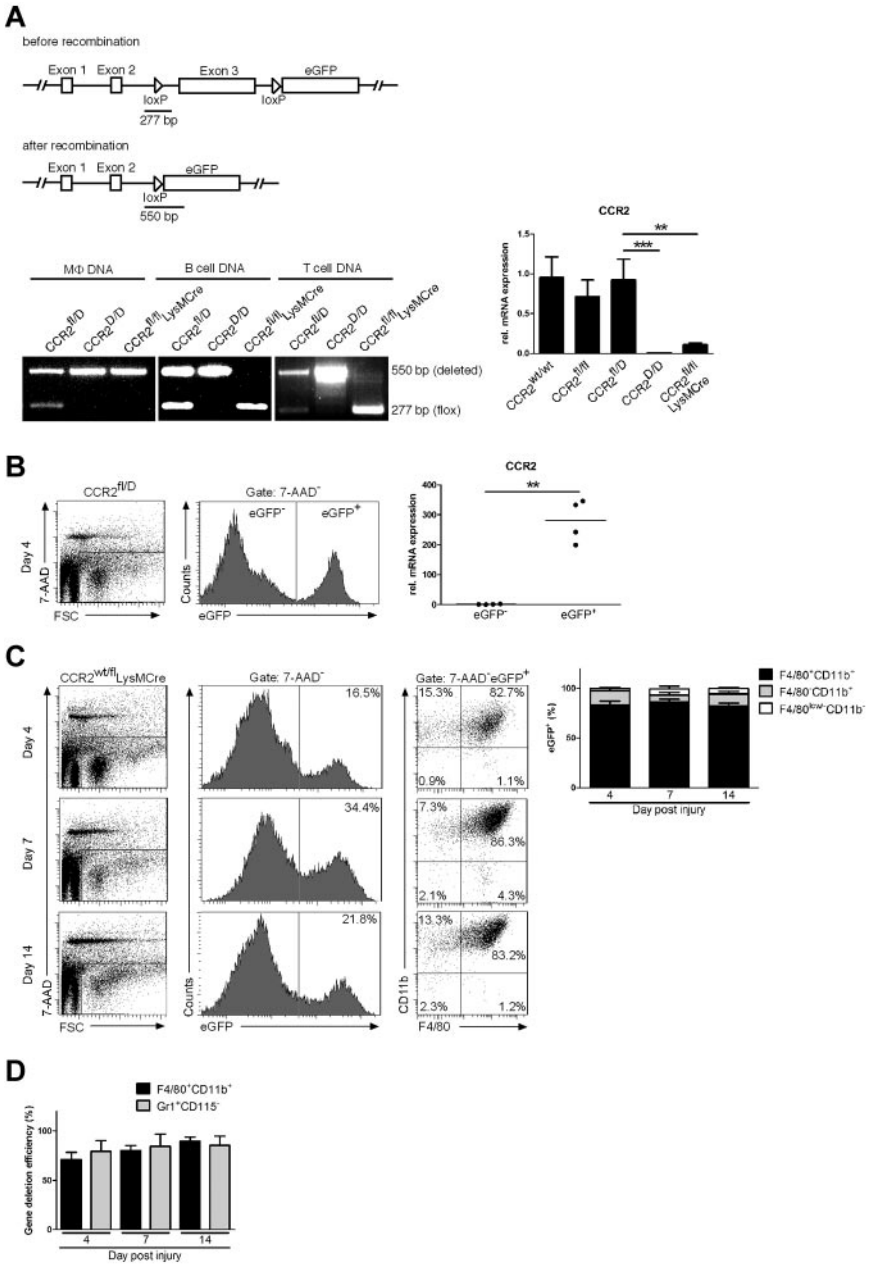

Figure 1. Conditional targeting of the *CCR2* gene. (A) Top, scheme illustrating the *CCR2* gene construct and the 2 loxP sites flanking exon 3, the eGFP cassette, and the PCR fragment length before and after successful recombination. Bottom left, PCR of genomic DNA isolated from various cell types and mouse mutants. Bottom right, relative expression of CCR2 in F4/80$^+$ cells FACS sorted from the peritoneal cavity in diverse mouse mutants (n = 3 mice per genotype). (B) Fidelity of reporter expression in CCR2$^{fl/D}$ mice: eGFP$^+$ and eGFP$^-$ wound cells were sorted for analysis of CCR2 mRNA expression (n = 4 wounds on 2 mice). (C) Specificity of LysMCre-mediated *CCR2* gene deletion in myeloid wound cells isolated from CCR2$^{wt/fl}$LysMCre mice: eGFP$^+$ cells were gated and analyzed for expression of F4/80 and CD11b at different time points after injury (n = 6-8 wounds on 2-3 mice per time point). (D) Efficiency of LysMCre-mediated *CCR2* gene deletion in myeloid wound cells: the frequency of eGFP$^+$ cells within the gates of F4/80$^+$CD11b$^+$ and Gr1$^+$CD115$^-$ cells isolated from wound tissues of CCR2$^{wt/fl}$LysMCre mice were determined and correlated with the frequency of eGFP$^+$ cells within the gates mentioned above isolated from wound tissue of CCR2$^{fl/D}$ mice (n = 6-8 wounds on 2-3 mice per time point). Two independent experiments were performed and data are expressed as means ± SD. $^{**}P < .01$; $^{***}P < .001$.

(JVC) at various magnifications (Leica DM4000B, Leica Microsystems; Diskus 4.50 Software, Diskus), as described previously.[3] Briefly, the extent of granulation tissue formation was determined and the gap between the epithelial tips was determined as a measure of wound closure. Objectives used at the Leica Microscope: 5×, NA 0.15; 10×, NA 0.4; and 40×, NA 0.75. Staining for CD31, Desmin, Dll4, and αSMA was quantified in high-power fields (7000 × 5500 μm^2) within granulation tissue using ImageJ software and a Nikon Eclipse 800E microscope (NIS-Elements AR 2.30 software, DXM 1200F digital camera). Objectives used at the Nikon microscope: 10×, NA 0.45 and 20×, NA 0.75. Analyses were performed in a blinded manner by 2 independent investigators. Images were processed with Adobe Photoshop Version 7.0 software.

Statistical analysis

Statistical analyses were performed using Prism Version 5 software (GraphPad). Significance of difference was analyzed with a Student paired or unpaired 2-tailed *t* test and ANOVA 1-way test analysis with a Dunnett multiple comparison test. In cases of variances that were not assumed to be equal, a Welch correction was performed. Data are presented as means ± SD. $P < .05$ was considered significant.

Results

Mouse models of complete or myeloid cell–restricted CCR2 gene inactivation and CCR2-eGFP reporter mice

To examine the expression and function of CCR2 for monocyte/macrophage recruitment into injured tissue, in the present study, we created a new Cre-loxP technology–based mouse model that could be used as CCR2-eGFP reporter mice or for complete or myeloid cell–restricted *CCR2* gene deletion. A detailed description of the generation of the CCR2^{fl}-eGFP mice will be provided elsewhere

(G.v.L. and M.P., manuscript in preparation). In brief, the *CCR2* allele was mutated by the insertion of 2 loxP sites flanking exon 3 (containing the entire coding sequence of *CCR2*), followed by an eGFP cassette (Figure 1A). Cre-mediated recombination deletes exon 3, resulting in a functional knockout of *CCR2*. At the same time, Cre-mediated deletion of exon 3 activates the expression of eGFP under the control of the endogenous *CCR2* locus. Therefore, eGFP is expressed from the null *CCR2* allele after Cre recombination, but is not expressed from the functional *CCR2* floxed allele. To generate mice of complete ($CCR2^{D/D}$) or myeloid cell–restricted ($CCR2^{fl/fl}$LysMCre) *CCR2* gene inactivation and CCR2-eGFP reporter mice ($CCR2^{fl/D}$), $CCR2^{fl/fl}$ mice were bred to corresponding Cre-strains (see "Methods" and supplemental Figure 1). Cre-mediated recombination was verified by PCR analysis of genomic DNA extracted from different cell types in diverse mouse mutants (Figure 1A bottom left). Efficiency of *CCR2* gene deletion in macrophages was examined by qRT-PCR in F4/80$^+$ cells FACS sorted from the peritoneal cavity in diverse mouse mutants (Figure 1A bottom right). The CCR2 transcript is attenuated significantly in F4/80$^+$ cells from $CCR2^{D/D}$ and $CCR2^{fl/fl}$LysMCre mice compared with $CCR2^{wt/wt}$, $CCR2^{fl/fl}$, and $CCR2^{fl/D}$ mice, in which the transcript is equivalent.

CCR2 expression was monitored in CCR2-eGFP reporter mice ($CCR2^{fl/D}$). To address the fidelity of reporter expression, excision skin wounds were inflicted on the backs of $CCR2^{fl/D}$ mice and single-cell suspensions of wounded tissues 4 days after injury were analyzed by flow cytometry. eGFP$^+$ and eGFP$^-$ cells were FACS sorted and qRT-PCR analysis showed that CCR2 mRNA expression was highly consistent with eGFP$^+$ cells (Figure 1B).

For myeloid cell–restricted *CCR2* gene deletion, $CCR2^{fl/fl}$ mice were bred to mice expressing Cre recombinase under the control of the myeloid cell–specific lysozyme M promoter ($CCR2^{fl/fl}$LysMCre).[23] To analyze the specificity and efficiency of LysMCre-mediated gene deletion, myeloid cell–restricted CCR2-eGFP reporter mice were generated ($CCR2^{wt/fl}$LysMCre). The specificity of LysMCre-mediated gene deletion at the wound site was analyzed by characterizing the fraction of eGFP$^+$ cells in single-cell suspensions of wound tissue from $CCR2^{wt/fl}$LysMCre reporter mice. For this purpose, excision skin wounds were inflicted on the backs of $CCR2^{wt/fl}$LysMCre mice and single-cell suspensions of wounded tissues during the early (day 4 after injury), middle (day 7 after injury), and late (day 14 after injury) phases of repair were analyzed by flow cytometry. During the entire time course of the healing response, F4/80$^+$CD11b$^+$ cells (tissue macrophages) represented the major fraction of eGFP$^+$ wound cells (mean over the entire time course, 84.2% ± 3.1%), followed by a minor fraction of F4/80$^-$CD11b$^+$ cells (polymorphonuclear leukocytes; mean over the entire time course, 11.0% ± 2.9%) and nonmyeloid F4/80$^{low/-}$CD11b$^-$ cells (mean over the entire time course, 4.7% ± 1.5%; Figure 1C). To assess the efficiency of LysMCre-mediated gene deletion at the wound site, we made use of the fact that in $CCR2^{wt/fl}$LysMCre mice, eGFP expression depends on Cre-mediated recombination under control of the lysozyme M promoter and subsequent activation of the *CCR2* promoter, whereas in $CCR2^{fl/D}$ mice, eGFP expression is independent of Cre recombinase activity and is solely regulated by *CCR2* promoter activity. Assuming an equal regulation of the *CCR2* promoter in both mouse lines, the efficiency of LysMCre-mediated gene deletion at the wound site was assessed by correlating the frequency of eGFP$^+$ myeloid wound cells in $CCR2^{wt/fl}$LysMCre reporter mice with the frequency of eGFP$^+$ myeloid wound cells in $CCR2^{fl/D}$ reporter mice (Figure 1D and supplemental Figure 3). The efficiency of *CCR2* gene deletion in F4/80$^+$CD11b$^+$ and Gr1$^+$CD115$^+$ (polymorphonuclear leukocytes) cells reached at least 71%, and slightly increased during healing progression: in F4/80$^+$CD11b$^+$ cells, 71.0% ± 7.3% at day 4, 80.2% ± 5.1% at day 7, and 89.5% ± 4.4% at day 14; in Gr1$^+$CD115$^+$ cells, 79.4% ± 10.9% at day 4, 84.6% ± 12.3% at day 7, and 89.4% ± 9.5% at day 14 (Figure 1D). These data demonstrate a high specificity and efficiency for *CCR2* gene deletion in myeloid cells present at the wound site of $CCR2^{wt/fl}$LysMCre mice.

Skin injury induces rapid accumulation of inflammatory CCR2$^+$Ly6C$^+$ monocytes/macrophages

To characterize tissue monocytes/macrophages during different stages of skin repair phenotypically, full-thickness excision skin wounds were inflicted on the backs of CCR2-eGFP reporter mice ($CCR2^{fl/D}$). Single-cell suspensions of wound tissues during the various phases of repair were analyzed by flow cytometry. During the early phase of the healing response, tissue macrophages (F4/80$^+$CD11b$^+$) comprised approximately one-quarter of all cells present at the wound site (23.5% ± 4.4%); their fraction increased significantly during the mid-phase (41.3% ± 3.1%) and declined to approximately one-third during the late phase of repair (34.3% ± 7.7%; Figure 2A). During healing progression, the F4/80$^+$CD11b$^+$ cell population revealed a distinct kinetic of diverse subpopulations (P1-P6) based on their eGFPLy6C (indicating CCR2Ly6C) profile (Figure 2A). Whereas eGFP^{hi}Ly6C^{hi} (P2) and eGFP^{hi}Ly6C$^{low/-}$ (P1) cells dominated the early healing stage and were associated with vascular sprouting/tissue growth, eGFP$^{med/low}$Ly6C$^{low/-}$ (P3) and eGFP$^-$Ly6C$^{low/-}$ (P5) cells dominated the late phase of tissue maturation and were associated with myofibroblast differentiation/matrix deposition (Figure 2B). Furthermore, analysis of the forward scatter/sideward scatter (FSC/SSC) profile revealed a monocytic phenotype of the subpopulation P1 at day 4 after injury (medium cell size and low granularity), whereas the subpopulations P3 and P5 at day 14 after injury revealed a rather mature macrophage phenotype (large cell size and high granularity; supplemental Figure 4). Fractions of eGFP$^{med/low}$Ly6C^{hi} (P4) and eGFP$^-$Ly6C^{hi} (P6) cells were minor over the entire time course of healing.

Early and late wound macrophages reveal distinct gene-expression profiles

To investigate whether wound macrophages are characterized by a distinct gene-expression profile during healing progression, single-cell suspensions of F4/80$^+$CD11b$^+$ cells were FACS sorted from wound tissue of wild-type mice and subjected to gene-expression analysis by qRT-PCR analysis. Gene expression of wound monocytes/macrophages was correlated with gene expression in circulating blood monocytes (SSC^{low}CD115$^+$CD11b$^+$) FACS sorted from unwounded mice. Wound monocytes/macrophages present during the early phase of repair revealed a gene-expression profile characterized by high expression of inflammatory mediators such as IL-6, inducible nitric oxide synthase (iNOS), and IL-1β (Figure 2C). This macrophage population was also characterized by strong expression of proangiogenic factors, including VEGF-A (henceforth referred as to VEGF) and Placental Growth Factor (PlGF), as well as Arginase-1. Expression of the majority of inflammatory, proangiogenic mediators, and Arginase-1 declined substantially during healing progression (Figure 2C). Expression of other genes, including IL-10, the scavenger receptor CD163, and the mannose receptor II (CD206), was low during the early phase but increased significantly during the late stage of repair (Figure 2C). In addition, we investigated whether the kinetics of wound macrophage

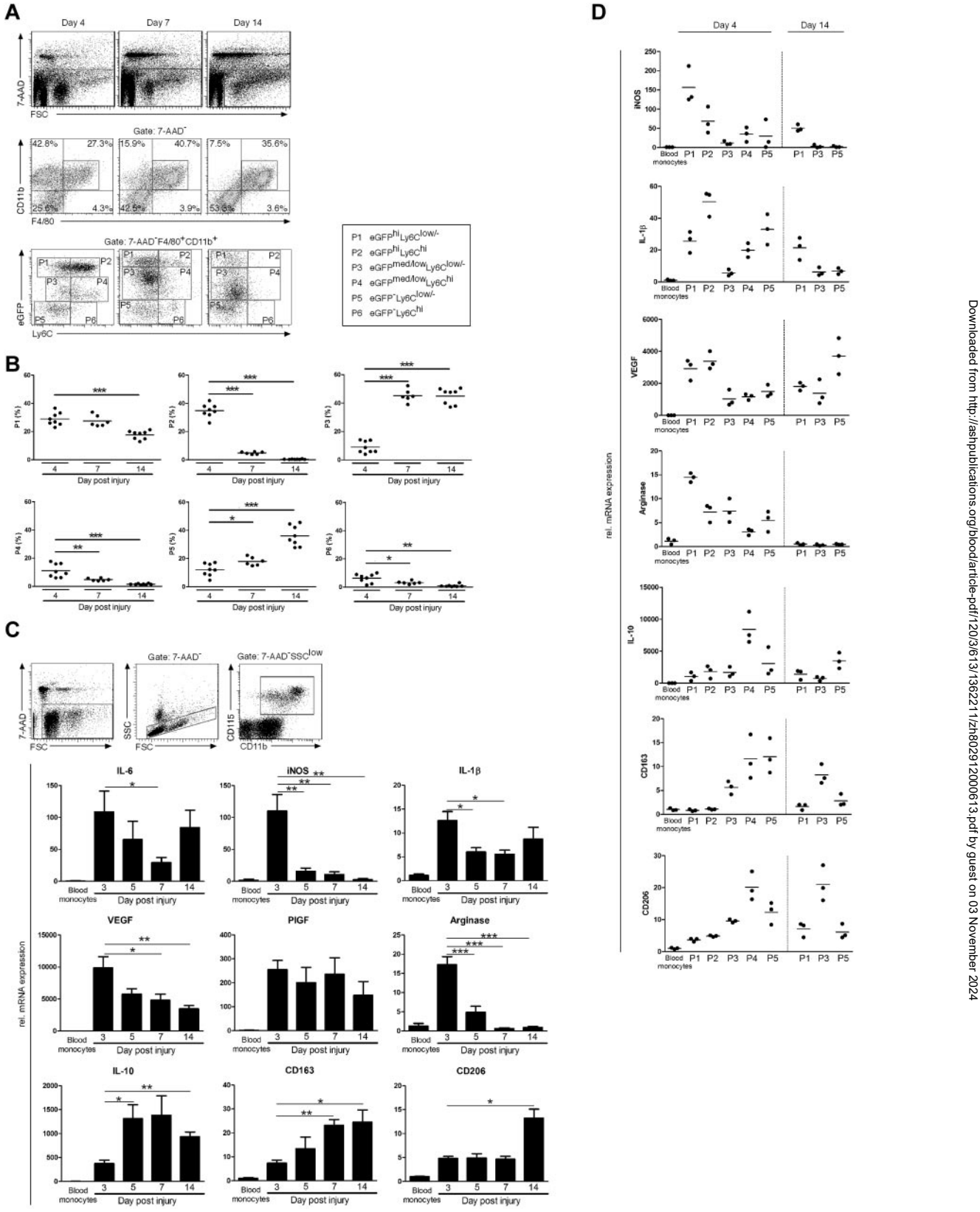

Figure 2. Skin injury induces the rapid accumulation of inflammatory CCR2$^+$Ly6C$^+$ monocytes/macrophages. (A) Representative FACS analysis of single-cell suspensions of wound tissue from CCR2$^{fl/D}$ mice at different time points after injury. F4/80$^+$CD11b$^+$ cells were gated and analyzed for expression of eGFP and Ly6C. (B) Fractions P1-P6 were gated and quantified (n = 6-10 wounds on 2-5 mice per time point). (C) Top, SSC^{low}CD11b$^+$CD115$^+$ blood monocytes were gated and FACS sorted for qRT-PCR analysis. Bottom, qRT-PCR analysis of selected genes in F4/80$^+$CD11b$^+$ macrophages isolated from wound tissue of control mice at different time points after injury normalized to gene expression in SSC^{low}CD11b$^+$CD115$^+$ blood monocytes (n = 4-8 wounds on 2-4 mice per time point). (D) qRT-PCR analysis of selected genes in F4/80$^+$CD11b$^+$ macrophages gated for P1-P6 fractions isolated from wound tissue in CCR2$^{fl/D}$ mice at different time points after injury and normalized to gene expression in SSC^{low}CD11b$^+$CD115$^+$ blood monocytes. Each dot represents 1 mouse (tissues of 4 wounds per mouse were pooled). A minimum of 2 independent experiments were performed and data are expressed as means ± SD. *$P < .05$; **$P < .01$; ***$P < .001$.

CCR2Ly6C phenotypes is linked to distinct gene-expression profiles (Figure 2D). These studies revealed that, based on their CCR2Ly6C profile, early and late macrophage populations are characterized by diverse gene-expression profiles. Whereas during the early phase of repair, the P1 and P2 populations exhibited a robust up-regulation of iNOS, IL-1β, VEGF, and Arginase-1, populations P4 and P5 exhibited a strong up-regulation of IL-10, CD163, and CD206. During the late stage of repair, the P3 or P5 populations in particular exhibited up-regulation of IL-10, CD163, CD206, or VEGF, whereas the inflammatory mediators were clearly down-regulated.

Interestingly, the F4/80$^+$CD11b$^+$ cells present during the early stage of repair combined a high level of iNOS and Arginase-1 expression (Figure 2C), which has been reported previously to be a characteristic for myeloid-derived suppressor cells (MDSCs).[26] To address the question of whether early wound tissue contains MDSCs, we analyzed single-cell suspensions from wounds at day 3 after injury by flow cytometry for the presence of MDSCs. This fraction of F4/80$^+$CD11b$^+$ cells contained a Ly6G$^-$Ly6C^{hi}eGFP^{hi} subset that may represent the monocytic fraction of MDSCs (supplemental Figure 5). However, gene-expression analysis revealed that it was not the eGFP^{hi}Ly6C^{hi} fraction (P2), but rather the eGFP^{hi}Ly6C$^{low/-}$ fraction (P1) of F4/80$^+$CD11b$^+$ cells that combined high levels of iNOS and Arginase-1 expression (Figure 2D). Therefore, it is unlikely that the monocytic fraction of MDSCs is present during the early repair phase in excision wounds. Within the fraction of F4/80$^-$CD11b$^+$ cells, Ly6G$^+$Ly6C^{med} cells could be identified, which may represent the granulocytic subset of MDSCs (supplemental Figure 5). However, further functional analysis would be required to distinguish these cells from polymorphonuclear cells, which are well known to be present abundantly during the early repair phase.

CCR2 is critical for the recruitment of blood CCR2$^+$Ly6C$^+$ monocytes/macrophages into skin wounds

Based on the finding that during the early phase of repair the majority of all F4/80$^+$CD11b$^+$ cells is CCR2$^+$ (Figure 2A), we speculated that the inflammatory CCR2$^+$Ly6C$^+$ blood monocyte subset is recruited predominantly to the site of skin injury and that CCR2 is functionally relevant for this process. As revealed by FACS analysis of single-cell suspensions of wounded tissues, up to day 7 after injury, the absolute number and the fraction of macrophages were reduced significantly in CCR2$^{D/D}$ and CCR2$^{fl/fl}$LysMCre mice compared with control mice (CCR2$^{fl/D}$; Figure 3A). Furthermore, in control mice, the dynamics of CCR2$^+$ cell recruitment was correlated with strong induction of the CCR2 ligand CCL2 at the wound site (Figure 3B). Levels of CCL2 expression at the wound site were similar in control and *CCR2* deleted mouse lines, indicating that induction of CCL2 expression is independent of macrophage invasion.

Whereas in unwounded CCR2$^{D/D}$ mice the number of circulating blood monocytes was reduced significantly compared with control mice, in CCR2$^{fl/fl}$LysMCre mice, this number was similar to controls (Figure 3C). CCR2 has been reported to be critical for monocyte progenitors to emigrate from the BM into the blood circulation,[27] and monocytopenia has complicated findings in CCR2-deficient mouse models used previously.[28,29] Consistent with earlier reports,[30] in the present study, we showed that LysMCre-mediated recombination was low in BM precursors (29.6% ± 5.0%) and increased in circulating blood monocytes (65.7% ± 4.9%), therefore enabling the majority of monocyte precursors to express the CCR2 required to egress from the BM (Figure 3D and supplemental Figure 6).

To substantiate the functional role of CCR2 for monocyte recruitment onto skin wounds, circulating blood monocytes of unwounded and wounded CCR2-eGFP reporter mice were analyzed by FACS analysis. Six hours after injury, the fraction of CCR2$^+$Ly6C$^+$ monocytes was reduced significantly compared with blood of unwounded mice and mice 12 days after injury (Figure 3E). Furthermore, the quantification of absolute numbers of CCR2$^+$Ly6C$^+$ circulating blood monocytes before injury ($3.1 \times 10^5 \pm 0.3 \times 10^5$) and 6 hours after injury ($0.6 \times 10^5 \pm 0.1 \times 10^5$), as well as determination of CCR2$^+$ cells at the wound site ($2.9 \times 10^5 \pm 0.4 \times 10^5$ in 4 wounds/mouse at day 4 after injury), supports the trafficking of CCR2$^+$Ly6C$^+$ blood monocytes to the wound site. In contrast, the fraction of CCR2$^-$Ly6C$^-$ monocytes was not reduced in the blood of unwounded and wounded mice during all stages after injury (Figure 3E). These findings suggest trafficking of CCR2$^+$Ly6C$^+$ blood monocytes to the wound site during the early phase of repair.

CCR2$^+$ blood monocytes recruited into skin wounds give rise to proangiogenic macrophages and initiate tissue vascularization

To investigate whether CCR2-mediated recruitment of monocytes/macrophages into the wound site is critical for the differentiation of proangiogenic macrophages, full-thickness skin wounds were inflicted on the backs of CCR2 mutants and control (CCR2$^{fl/D}$) mice. At various time points after injury, wound angiogenesis and the development of granulation tissue were examined by histology. Quantitative analysis of H&E- and CD31-stained wound sections showed that the amount and, particularly, the vascularization of granulation tissue was reduced significantly during the early and middle stages of repair in both complete and myeloid cell–restricted *CCR2*-knockout mice compared with controls (Figure 4A-D). Increased VEGF expression in F4/80$^+$CD11b$^+$eGFP$^+$ isolated wound cells (Figure 4E) and reduced VEGF expression in complete wound tissue in *CCR2*-knockout mice (Figure 4F) indicated that CCR2-recruited wound macrophages provide a significant source of VEGF transcript at the site of skin injury. Immunohistochemical analysis for αSMA expression, the signature mediator for myofibroblast differentiation, in wounds of CCR2$^{fl/fl}$LysMCre and CCR2$^{D/D}$ mice revealed transiently reduced staining at the early and middle phases of repair compared with controls (Figure 4G). As assessed by Sirius red staining and analysis by polarized light, the organization, distribution, and fibrillar structure of collagen fibers in scar tissue at day 14 after injury was similar in controls and *CCR2*-deleted mice (data not shown). The rate of wound closure was not affected by *CCR2* deletion (Figure 4D). Overall, these findings suggest that in excision skin wounds in mice, CCR2-mediated recruitment of blood monocytes into the wound site is critical for establishing tissue vascularization and myofibroblast differentiation during the early stages of repair, whereas scar formation appears to be independent of this process.

Macrophages are the prevailing VEGF source during the early phases of tissue repair

To analyze in more detail the functional role of monocyte/macrophage–derived VEGF during skin-wound healing, we characterized VEGF-expressing cell types during the diverse stages of the healing response. Earlier wound-healing studies in different transgenic VEGF reporter mouse lines have yielded contradictive results.[31,32] In the present study, we inflicted full-thickness skin

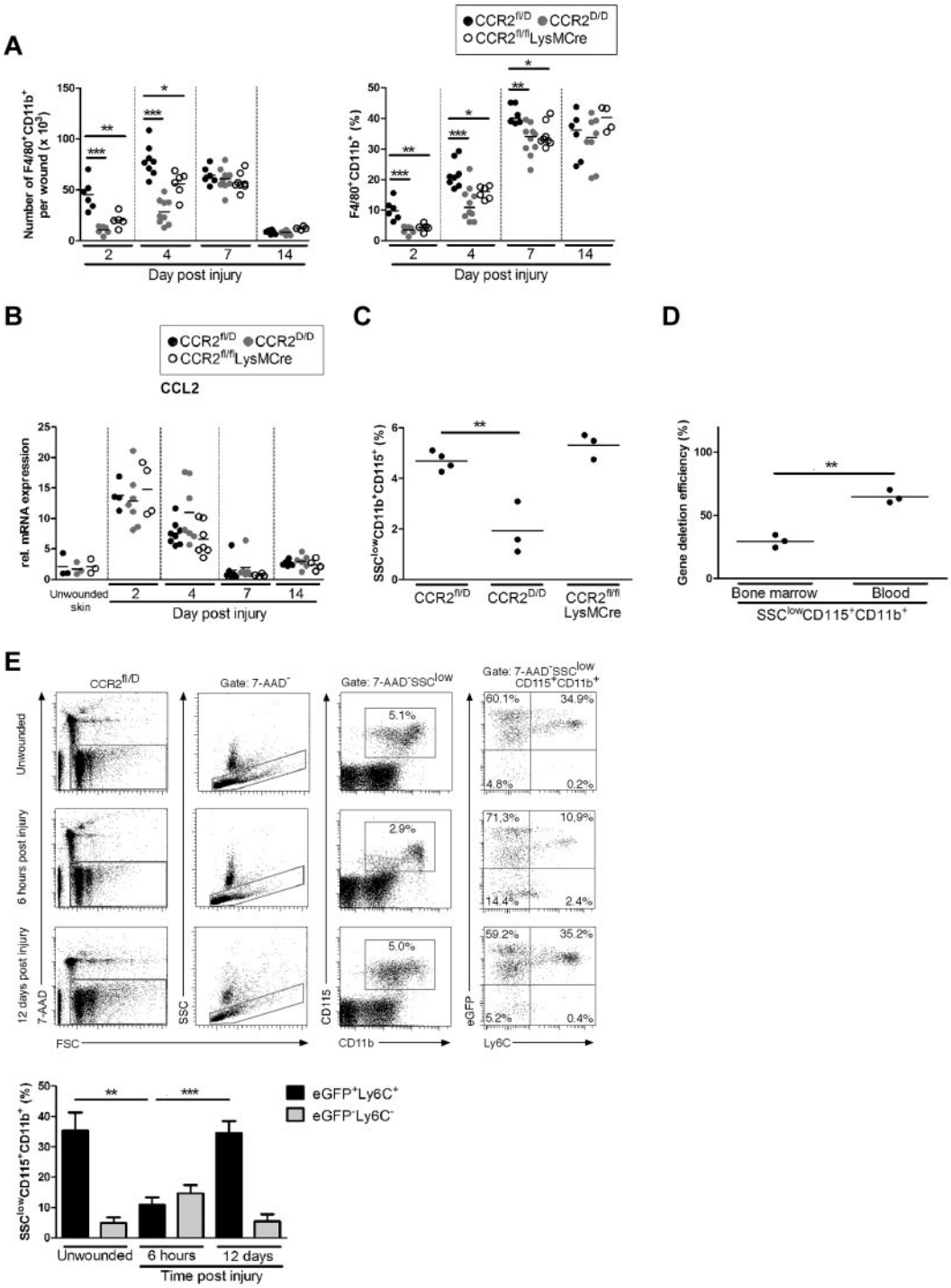

Figure 3. CCR2 is critical for homing of inflammatory monocytes to skin wounds. (A) Absolute cell number (left) and fraction of F4/80$^+$CD11b$^+$ cells (right) in wound tissue of different mutants were determined by FACS analysis (n = 6-10 wounds on 2-5 mice per time point). (B) qRT-PCR analysis for CCL2 in wound tissue from mutants at different time points after injury normalized to unwounded skin. (C) Fractions of SSC^{low}CD11b$^+$CD115$^+$ blood monocytes in unwounded mutants were determined by FACS analysis. (D) Efficiency of LysMCre-mediated *CCR2* gene deletion in monocyte precursors/monocytes isolated from BM and blood. Frequency of eGFP$^+$ cells within the gate of SSC^{low}CD11b$^+$CD115$^+$ cells isolated from CCR2$^{wt/fl}$LysMCre mice were determined and correlated with the frequency of eGFP$^+$ cells within the gate mentioned above isolated from CCR2$^{fl/D}$ mice. (E) Representative FACS analysis of PBMCs isolated from CCR2$^{fl/D}$ mice before and after injury. SSC^{low}CD11b$^+$CD115$^+$ cells were gated and analyzed for the expression of eGFP and Ly6C (n = 3-4 mice per time point). In panels A and B, each dot represents 1 wound; in panels C and D, each dot represents 1 mouse. A minimum of 2 independent experiments were performed and data are expressed as means ± SD. *$P < .05$; **$P < .01$; ***$P < .001$.

wounds on the backs of VEGF-lacZ knock-in reporter mice,[33] and wound tissue was subjected to β-galactosidase staining. Whereas unwounded skin revealed only few VEGF-expressing cells within the subcutaneous fat, skin injury resulted in a robust increase of VEGF expression (Figure 5A). Morphologic and FACS analyses revealed a dynamic switch between macrophages being the prevailing VEGF source during the early healing stage and, as healing progressed, the developing neoepithelium at the wound edge

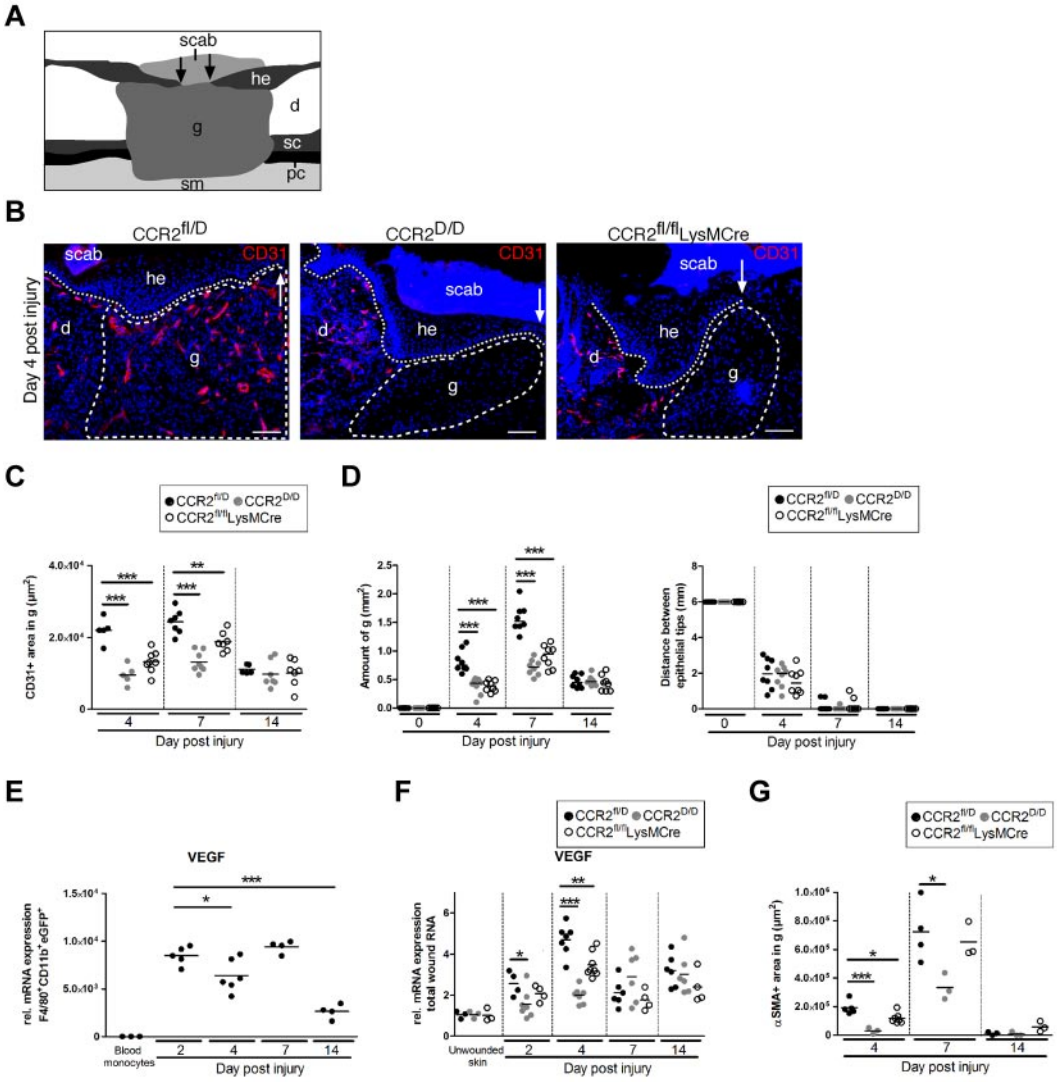

Figure 4. CCR2 is critical for the recruitment of proangiogenic monocytes/macrophages into skin wounds. (A) Scheme illustrating skin wound histology. (B-D) CD31 immunostaining (B) and morphometric quantification of CD31-stained (C) or H&E-stained (D) wound tissue at different time points after injury. (E-F) qRT-PCR analysis for VEGF in F4/80$^+$CD11b$^+$eGFP$^+$ macrophages isolated from CCR2$^{fl/D}$ mice normalized to expression in SSC^{low}CD11b$^+$CD115$^+$ blood monocytes (E) and in wound tissue from mutants at different time points after injury normalized to unwounded skin (F). (G) Morphometric quantification of αSMA-stained wound tissue of the indicated mouse strains. Three independent experiments were performed and each dot represents 1 wound. Hatched line indicates granulation tissue; dotted line, hyperproliferative epithelial tongue; arrows, tip of epithelial tongue; d, dermis; g, granulation tissue; he, hyperproliferative epithelium; sc, subcutaneous fat tissue; pc, panniculus carnosus; and sm, skeletal muscle. Bars indicate 100 μm. *$P < .05$; **$P < .01$; ***$P < .001$.

during the late stage (Figure 5A-B and supplemental Figure 7A). Unexpectedly, although F4/80$^+$CD11b$^+$ macrophages represented the prevailing cell source expressing VEGF during the early phase of repair, only a small fraction of all macrophages present at the wound site expressed VEGF (F4/80$^+$FDG$^+$, 19.1% ± 2.1% at day 4 after injury; Figure 5C and supplemental Figure 7B).

VEGF-expressing macrophages reveal a mixed M1/M2 phenotype

To examine the activation state of VEGF-expressing macrophages infiltrating the wound site, VEGF-expressing (F4/80$^+$FDG$^+$) and VEGF-negative cells (F4/80$^+$FDG$^-$) were isolated from wound tissues of VEGF-lacZ reporter mice, FACS sorted, and analyzed for M1 and M2 gene-expression profiles by qRT-PCR analysis (Figure 5D and supplemental Figure 7C). During the early phase of repair, VEGF-expressing macrophages revealed a significant up-regulation of the proinflammatory mediators IL-6 and iNOS and less pronounced expression of the M2 marker Arginase-1 compared with VEGF-negative macrophages (Figure 5D). Interestingly, the cell-surface marker Tie2, a hallmark of a tumor-associated M2-like monocyte subset with strong proangiogenic activities,[9,34] was substantially up-regulated in VEGF-expressing cells (Figure 5D). Other Tie2-expressing monocyte-related markers, including CD163 and Nrp1 (Figure 5D) and other known M1/M2 gene signatures (IL-1β, TNF-α, Fizz1, IL-10, and TGF-β1; data not shown), were not differentially expressed. Our findings show that VEGF-expressing wound macrophages share features of both M1 and M2 activation.

Myeloid cell–derived and epidermal-derived VEGF have unique and complementary functions during wound vascularization

To analyze the functional impact of myeloid cell–derived VEGF synthesis in skin-wound healing, we generated mice with myeloid cell–specific *VEGF-A* deletion (VEGF$^{fl/fl}$LysMCre mice) and inflicted full-thickness wounds on their backs. For this purpose,

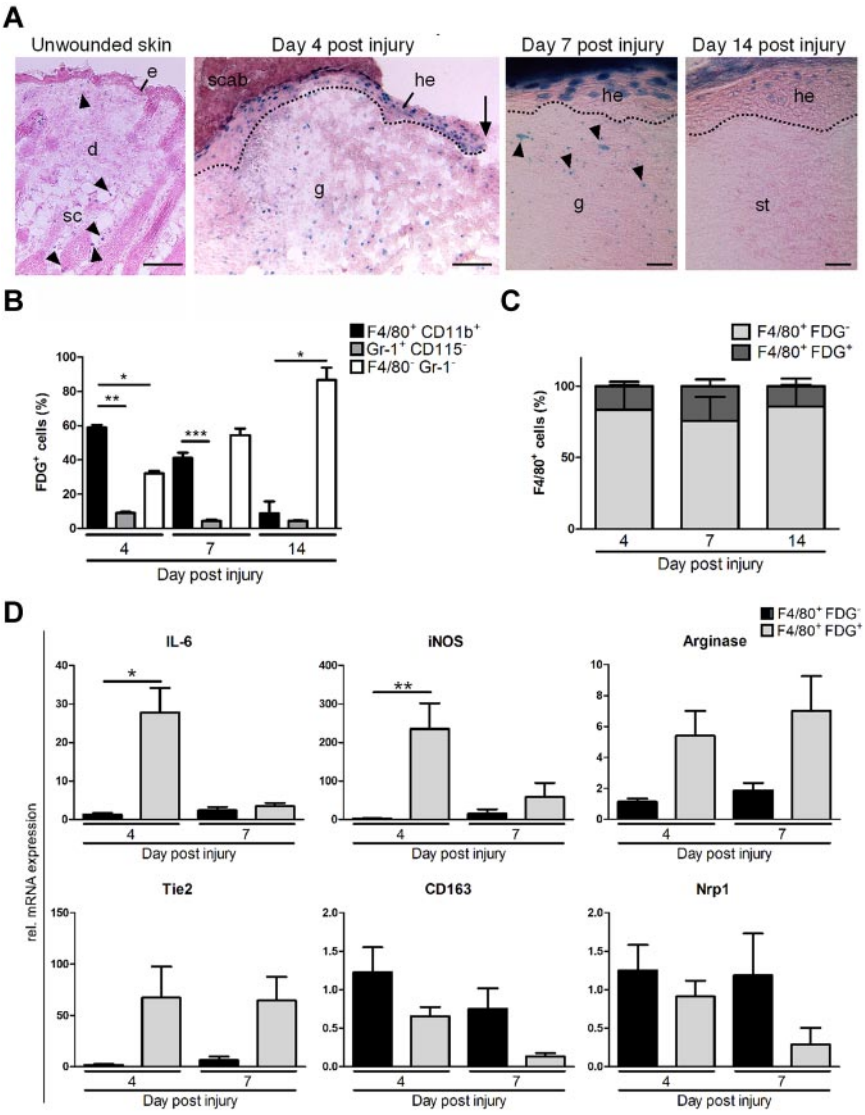

Figure 5. Macrophages are the prevailing VEGF source in the early phase of skin repair and demonstrate features of M1/M2 activation. (A) X-Gal staining of unwounded and wounded skin of VEGF-lacZ reporter mice. e indicates epidermis; d, dermis; sc, subcutaneous fat tissue; he, hyperproliferative epithelium; g, granulation tissue; st, scar tissue; pc, panniculus carnosus; sm, skeletal muscle; arrowheads, positive stained cells; dotted line, basement membrane; and arrow, tip of epithelial tongue; scale bars for unwounded skin and day 4, 100 μm; scale bars for day 7 and 14, 10 μm. (B) FDG^+ wound cells from VEGF-lacZ reporter mice were isolated, analyzed by FACS, and gated for macrophages ($F4/80^+CD11b^+$), neutrophils ($Gr\text{-}1^+CD115^-$), and non-myeloid cells ($F4/80^-Gr\text{-}1^-$). (C) Quantification of FACS-analyzed wound cells in VEGF-lacZ mice gated for $F4/80^+FDG^-$ and $F4/80^+FDG^+$ (n = 8-12 wounds on 2-3 mice per time point). (D) Relative expression of selected genes in $F4/80^+FDG^-$ and $F4/80^+FDG^+$ cells at different time points after injury (n = 3-6 mice per time point). Data are expressed as means ± SD. $^*P < .05$; $^{**}P < .01$; $^{***}P < .001$.

$VEGF^{fl/fl}$ mice[21] were crossed to LysMCre mice. The efficiency and myeloid cell specificity of Cre-mediated deletion was verified by various methods and was consistent with earlier studies[14] (supplemental Figure 8A-C). In addition, VEGF transcript in $F4/80^+CD11b^+$ cells FACS sorted from wound tissue in $VEGF^{fl/fl}$LysMCre mice was reduced significantly compared with controls (Figure 6A). Quantitative analysis of H&E-stained (Figure 6B and supplemental Figure 8D) and CD31/desmin-stained (Figure 6C-D) wound sections at various stages after skin injury showed that the amount, cellularity, and vascularization of granulation tissue was reduced significantly during the early phase of repair in $VEGF^{fl/fl}$LysMCre mice compared with controls and was rescued at later stages. These findings suggest nonredundant functions for myeloid cell–derived VEGF for the induction of wound angiogenesis. During the transition from the early to the middle stage of repair (day 7 after injury), vascularization in the wounds of $VEGF^{fl/fl}$LysMCre mice increased substantially and was excessive compared with control wounds ($P < .01$; Figure 6D), potentially by VEGF synthesis through other cell compartments. Our findings in wounded VEGF-lacZ reporter mice indicated that the neoepithelium dominates VEGF delivery during the late stage of skin repair (Figure 5A). Therefore, we generated mice lacking VEGF expression in both myeloid cells and the epidermal compartment. For this purpose, $VEGF^{fl/fl}$LysMCre mice were crossed to K14Cre mice, which have been reported to express Cre recombinase in basal keratinocytes ($VEGF^{fl/fl}$LysMCreK14Cre).[22] The efficiency of Cre-mediated deletion in the epidermis was verified by PCR analysis of DNA that was extracted from tail biopsies (supplemental Figure 9A). In addition, whereas in complete wound tissue of $VEGF^{fl/fl}$LysMCre mice, attenuated VEGF expression was limited to the early phase of repair (Figure 6E), in $VEGF^{fl/fl}$LysMCreK14Cre double-knockout mice, VEGF expression was also reduced at the later stages compared with controls (Figure 6F). Quantitative analysis of H&E-stained (Figure 6G and supplemental Figure 9B) and CD31/desmin-stained (Figure 6H and supplemental Figure 9C) wound sections showed that the formation and vascularization of granulation tissue was reduced substantially during both the early and middle phases of repair in double-knockout mice compared with controls. Immunohistochemical analysis for αSMA expression in wounds of $VEGF^{fl/fl}$LysMCre and $VEGF^{fl/fl}$LysMCreK14Cre mice revealed a transiently reduced αSMA staining at day 4 after injury compared with controls (Figure 6I). As assessed by Sirius red stain and analysis by polarized light, the organization, distribution, and fibrillar structure of collagen fibers in scar tissue at day 14 after injury were not altered by VEGF deletion (data not shown). Overall, these findings propose a dynamic and functionally relevant

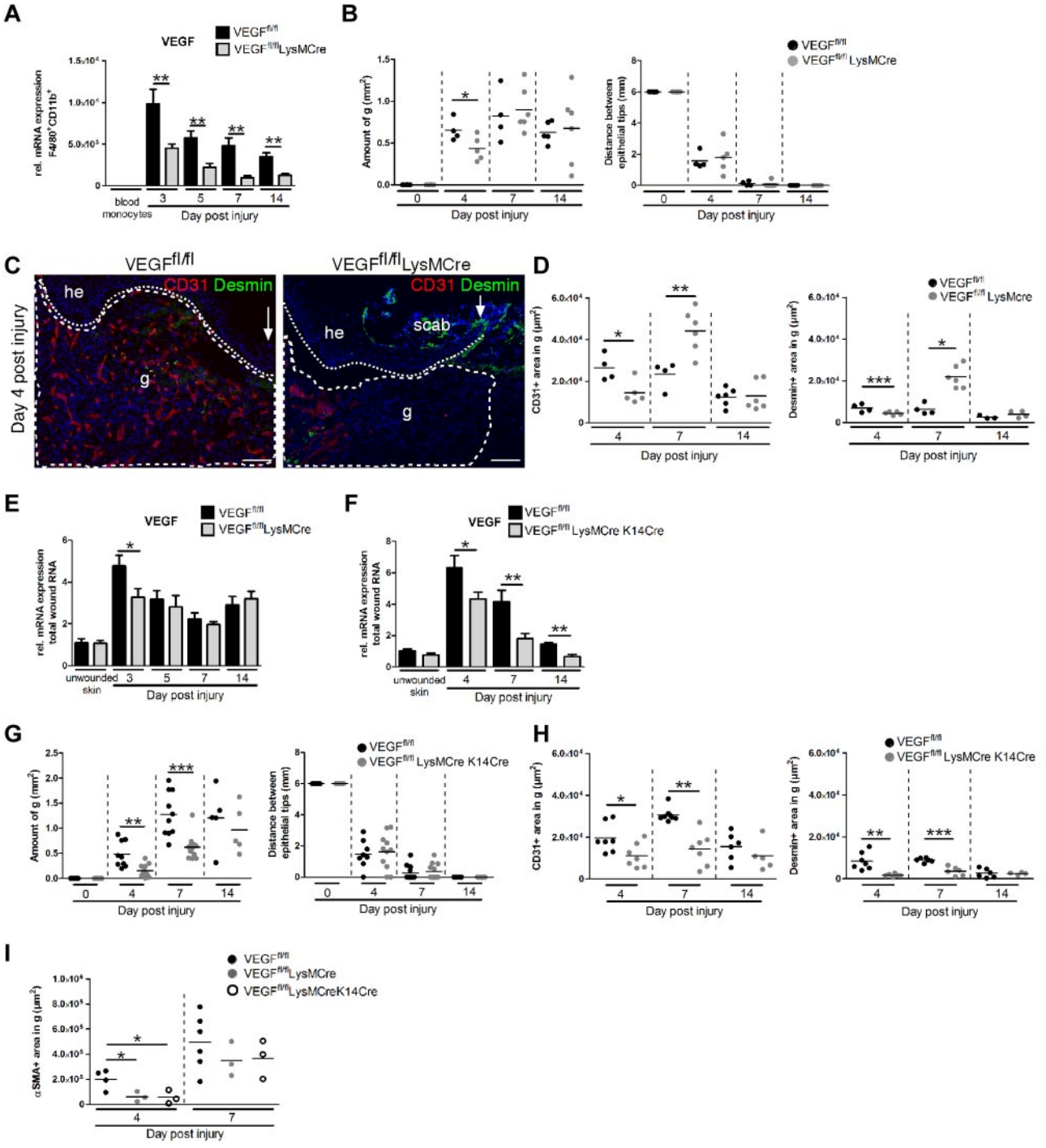

Figure 6. Myeloid cell–derived VEGF is critical for the induction of wound angiogenesis and tissue growth during the early phase of repair. (A) qRT-PCR analysis for VEGF in F4/80$^+$CD11b$^+$ macrophages isolated from wound tissue of mutants at different time points after injury normalized to SSC^{low}CD11b$^+$CD115$^+$ blood monocytes (n = 4-8 wounds on 2-4 mice per time point and genotype). (B) Morphometric analysis of H&E-stained wound tissue at different time points after injury. (C-D) CD31/desmin double immunostaining (C) and morphometric quantification (D) of wound tissue. (E) qRT-PCR analysis for VEGF expression in complete wound tissue at the indicated time points after injury normalized to unwounded skin (n = 4-8 wounds on 2-4 mice per time point). (F) qRT-PCR analysis for VEGF expression in complete wound tissue at the indicated time points after injury normalized to VEGF expression in unwounded skin (n = 4-8 wounds on 2-4 mice per time point). (G) Morphometric analysis of H&E-stained wound tissue. (H-I) Morphometric quantification of CD31/desmin double immunostained (H) or αSMA-stained (I) wound tissue. Data are expressed as means ± SD. Each dot represents 1 wound; hatched line, granulation tissue; dotted line, hyperproliferative epithelial tongue; arrows, tip of epithelial tongue; g, granulation tissue; and he, hyperproliferative epithelium. Scale bars indicate 100 µm. Three independent experiments were performed. *$P < .05$; **$P < .01$; ***$P < .001$.

interplay between myeloid- and epidermal-derived VEGF during skin repair that is critical for timely and effective wound angiogenesis and the development of granulation tissue. Although VEGF-deficient and control macrophages revealed differential expression of several proangiogenic genes when exposed to hypoxia in vitro (supplemental Figure 10), these differences could not be detected in the wound tissue of VEGF$^{fl/fl}$LysMCre mice (data not shown).

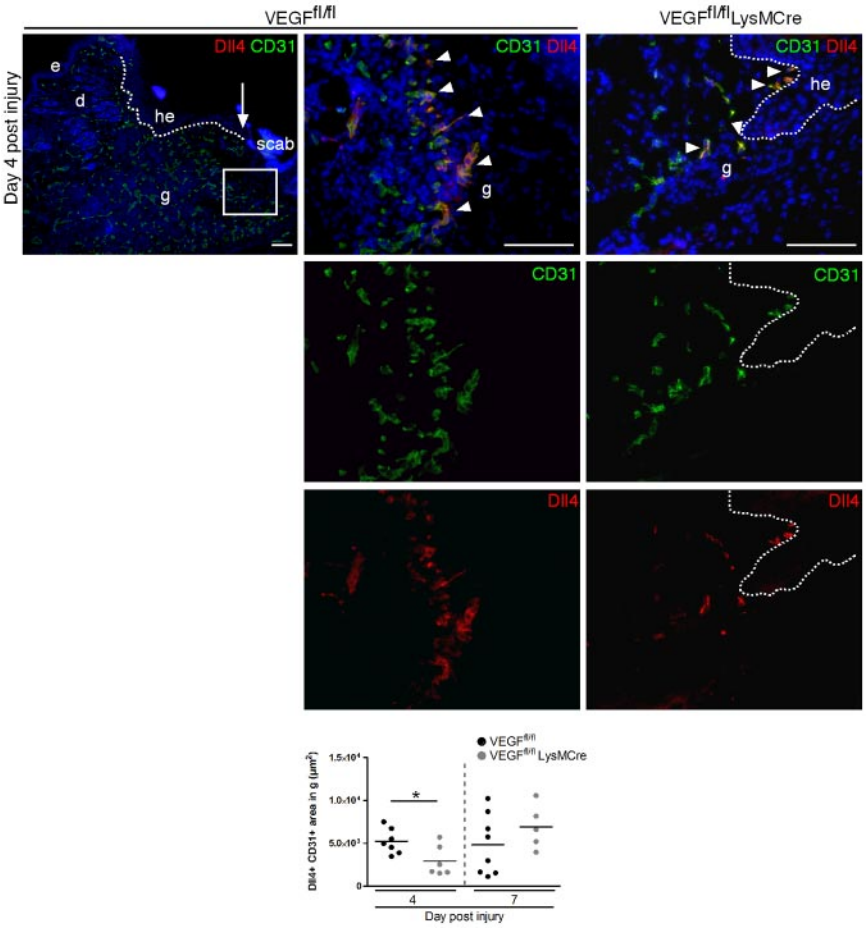

Figure 7. Macrophage-derived VEGF controls vascular sprout induction during the early phase of tissue repair. Shown are CD31/Dll4 double immunostaining and morphometric quantification of wound tissue. Left, rectangle outlines vascular structures within granulation that are presented at higher magnification in images presented in the middle. Arrow indicates the tip of epithelial tongue; dotted line, hyperproliferative epithelial tongue; arrowheads, front of sprouting tips; he, hyperproliferative epithelium; and g, granulation tissue. Scale bar indicates 100 μm. Three independent experiments were performed and each dot represents 1 wound. *$P < .05$.

Myeloid cell–derived VEGF controls induction of vascular sprouts during the early phase of tissue repair

To substantiate cellular mechanisms that potentially control macrophage-derived VEGF-mediated angiogenesis during the early phase of repair, we examined whether macrophage-derived VEGF is critical for the induction of Dll4$^+$ endothelial cells, a feature of tip cells.[35] Recently, it was shown that Dll4-Notch1 signaling regulates the formation of appropriate numbers of tip cells to control proper vessel sprouting and branching in the mouse retina in a VEGF-dependent fashion.[35,36] To our knowledge, the role of this mechanism in cutaneous wound angiogenesis has not yet been reported. In the present study, we show abundant CD31$^+$ vascular structures within the granulation tissue of day-4 wounds in control mice that advance from the wound periphery (wound edge) toward the scarcely vascularized wound center (Figure 7). However, double staining for Dll4 and CD31 was limited to cellular structures at the leading edge of vascular sprouts invading the provisional extracellular matrix at the center of the wound (Figure 7). In contrast, in wound tissue of VEGF$^{fl/fl}$LysMCre mice, only few Dll4$^+$ cells were detected within the poorly vascularized granulation tissue. These findings suggest that macrophage-derived VEGF is critical for the induction, and potentially protrusion, of Dll4$^+$ vascular sprouts during the early stage of granulation tissue formation in skin wounds.

Discussion

The role of phenotypic and functional plasticity of monocytes/macrophages in various disease conditions is currently under intensive investigation.[17] The possibility of manipulating tissue function by selectively targeting monocyte/macrophage subpopulations may give rise to novel monocyte-based therapies. However, at present, the challenge is to identify precisely the phenotype and functions of monocytes/macrophages attracted to the site of damaged tissue and to differentiate which of their signals are beneficial or harmful for restoration of tissue integrity. In the present study, we tested the hypothesis that distinct monocyte/macrophage phenotypes control the dynamics of diverse repair mechanisms after excision skin injury.

We show herein that whereas macrophages present during the late stage of repair predominantly provide an M2 gene-expression profile (ie, IL-10, CD163, and CD206), monocytes/macrophages present during the early stage of repair combine an up-regulation of both mediators that have been associated with M1 (ie, IL-6, iNOS, and IL-1β) and M2 (ie, Arginase-1, VEGF, PlGF, and Tie2) macrophage activation. Therefore, the present study may provide evidence as to why M1/M2 polarity nomenclature for macrophage differentiation in excision skin repair is not necessarily that useful. Furthermore, we show herein that CCR2 signaling is critical for the recruitment of Ly6C$^+$ inflammatory circulating blood monocytes into skin wounds, which give rise to a highly proangiogenic, VEGF-expressing macrophage subset with nonredundant functions for the induction of vascular sprouts and tissue growth during the early stage of the repair response.

The role of CCR2 in mediating homing of blood monocytes to inflamed tissues has been investigated intensively in various model systems,[37-39] but its specific function in this process is still

unclear.[28] Interpretation of findings in previously used CCR2 deficient mouse models has been complicated by the fact that reduced monocyte/macrophage numbers at the lesion may reflect monocytopenia.[27] In the present study, we show that, in contrast to complete *CCR2*-knockout mice, in LysMCre-mediated myeloid cell–restricted CCR2-deficient mice, the number of circulating blood monocytes is equivalent to that of control mice. LysMCre-mediated *CCR2* deletion is low in BM precursors and increased in circulating blood monocytes. Therefore, our findings in CCR2$^{fl/fl}$LysMCre mice strongly suggest that reduced monocytes/macrophages at the wound site are due to attenuated trafficking of blood monocytes into the damaged tissue and are not the result of reduced monocytes in the circulation. Furthermore, our findings propose that *CCR2* gene deletion under control of the myeloid cell–specific lysozyme M promoter offers a new, and likely superior, experimental model with which to investigate the role of CCR2 in monocyte homing.

Our present findings show a critical functional link between CCR2-mediated recruitment of Ly6C$^+$ circulating blood monocytes and initiation of tissue vascularization, tissue growth, and induction of myofibroblast differentiation, whereas the extent of scar formation and overall wound closure do not appear to be controlled by this process. Consistently, we and others have reported recently the abrogation of wound angiogenesis and myofibroblast differentiation after selective macrophage depletion during the early stage of skin repair.[3] Furthermore, in an experimental tumor model, it was shown recently that CCL2-CCR2 signaling is essential for the recruitment of inflammatory monocytes to metastasis, tumor vascularization, and the progression of tumor disease.[40] These findings support an important mechanistic link between CCR2-mediated monocyte recruitment and tissue vascularization in the context of both physiologic and pathologic tissue growth.

VEGF was one of the most prominent regulated genes among those analyzed in CCR2$^+$Ly6C$^+$ monocytes/macrophages present during the early wound-healing stage. Furthermore, abrogation of wound tissue vascularization in myeloid cell–restricted CCR2-deficient mice was paralleled by significant attenuation of VEGF expression. Therefore, we speculated that monocytes/macrophages at the early stage of repair initiate wound-tissue vascularization by a process that requires specifically monocyte/macrophage-derived VEGF. This assumption was supported by earlier wound-healing studies in mice with keratinocyte-restricted VEGF deficiency, which showed disturbed vascular growth particularly in late stage wound healing while angiogenesis during the early phase was not affected.[24] Examining a VEGF-lacZ reporter mouse line, in the present study, we identified 2 previously unrecognized findings regarding diverse cellular sources of VEGF within a single tissue: (1) a dynamic switch between macrophages as the prevailing VEGF source during the early phase of repair and the neoepithelium at later stages, and (2) functional macrophage heterogeneity in regenerating tissue.

Using conditional gene targeting, we have shown herein that both VEGF expression in myeloid cells per se and the switch of VEGF expression in the myeloid and epidermal cell compartments are critical mechanisms for a timely induction of capillary sprouts, physiologic dynamics of blood vessel formation, and tissue growth at the wound site. Myeloid cell–restricted VEGF deficiency prevented vessel sprouting during the early healing phase, but paradoxically led to an excessive vascular response in subsequent healing stages that was abrogated by simultaneous epidermal VEGF deficiency. Although, further experimental analysis is required to dissect the mechanisms of how alternative sources of VEGF act in concert to control the timely induction of vascular sprouts and the formation of a vascular network, overall, our present findings suggest a dynamic and functional complementary interplay between 2 different cell compartments that synthesize VEGF for effective vascularization and granulation tissue formation in skin wounds.

The results of the present study in skin corroborate the current evidence in other organs that in postnatal life, the recruitment of circulating blood monocytes into damaged tissue and the ensuing monocyte/macrophage activation are critical to establishing an effective healing response. Furthermore, we demonstrate herein a critical role for CCR2-mediated recruitment of Ly6C$^+$ inflammatory blood monocytes to initiate vascularization in a tissue-regenerative context. Unexpectedly, VEGF expression in a distinct inflammatory monocyte/macrophage subpopulation shortly after invasion was sufficient and vital for this process. Our findings suggest the hypothesis that the recruitment of CCR2$^+$Ly6C$^+$ inflammatory blood monocytes into ischemic tissues can be manipulated therapeutically to facilitate vascularization and tissue growth in healing-impaired disease states.

Acknowledgments

The authors thank Michael Piekarek and Margot Junker for preparing histologic sections, Christoph Göttlinger and Gunter Rappl for support in cell sorting, and Martin Hellmich for advice in statistical analysis.

This work was supported by a grant from the Deutsche Forschungsgemeinschaft (Sonderforschungsbereich 829 to S.A.E., T.K., M.P., I.H., and B.B.), by the European Union (Angioscaff NMP-LA-2008-214402 to S.A.E.), and the Europäischer Fond für Regionale Entwicklung program for Nordshein-Westfalen im Ziel 2 Regionale Wettbewerbsfähigkeit und Beschäftigung 2007-2013 (to S.A.E.). G.v.L. was supported by the Group-ID Multidisciplinary Research Partnership of Ghent University.

Authorship

Contribution: S.W., T.L., J.A.K., and S.A.E. analyzed the data; G.v.L. and M.P. generated the CCR2 mice; S.W., T.L., T.K., I.H., M.H., A.N., and S.A.E. wrote the manuscript; S.W., T.L., B.B., and S.A.E. designed and performed the research; A.N. generated the VEGF-lacZ mice; and N.F. generated the VEGF$^{fl/fl}$ mice.

Conflict-of-interest disclosure: The authors declare no competing financial interests.

Correspondence: Sabine Eming, MD, Professor of Dermatology, Department of Dermatology, University of Cologne, Kerpenerstr 62, 50937 Cologne, Germany; e-mail: sabine.eming@uni-koeln.de.

References

1. Gurtner GC, Werner S, Barrandon Y, Longaker MT. Wound repair and regeneration. *Nature.* 2008; 453(7193):314-321.
2. Duffield JS, Forbes SJ, Constandinou CM, et al. Selective depletion of macrophages reveals distinct, opposing roles during liver injury and repair. *J Clin Invest.* 2005;115(1):56-65.
3. Lucas T, Waisman A, Ranjan R, et al. Differential roles of macrophages in diverse phases of skin repair. *J Immunol.* 2010;184(7):3964-3977.
4. Pollard JW. Trophic macrophages in development and disease. *Nat Rev Immunol.* 2009;9(4):259-270.

5. Okuno Y, Nakamura-Ishizu A, Kishi K, Suda T, Kubota Y. Bone marrow-derived cells serve as proangiogenic macrophages but not endothelial cells in wound healing. *Blood.* 2011;117(19):5264-5272.
6. Murdoch C, Muthana M, Coffelt SB, Lewis CE. The role of myeloid cells in the promotion of tumour angiogenesis. *Nat Rev Cancer.* 2008;8(8):618-631.
7. Eming SA, Krieg T, Davidson JM. Inflammation in wound repair: molecular and cellular mechanisms. *J Invest Dermatol.* 2007;127(3):514-525.
8. Fantin A, Vieira JM, Gestri G, et al. Tissue macrophages act as cellular chaperones for vascular anastomosis downstream of VEGF-mediated endothelial tip cell induction. *Blood.* 2010;116(5):829-840.
9. Pucci F, Venneri MA, Biziato D, et al. A distinguishing gene signature shared by tumor-infiltrating Tie2-expressing monocytes, blood "resident" monocytes, and embryonic macrophages suggests common functions and developmental relationships. *Blood.* 2009;114(4):901-914.
10. Outtz HH, Wu JK, Wang X, Kitajewski J. Notch1 deficiency results in decreased inflammation during wound healing and regulates vascular endothelial growth factor receptor-1 and inflammatory cytokine expression in macrophages. *J Immunol.* 2010;185(7):4363-4373.
11. Outtz HH, Tattersall IW, Kofler NM, Steinbach N, Kitajewski J. Notch1 controls macrophage recruitment and Notch signaling is activated at sites of endothelial cell anastomosis during retinal angiogenesis in mice. *Blood.* 2011;118(12):3436-3439.
12. Stockmann C, Kirmse S, Helfrich I, et al. A wound size-dependent effect of myeloid cell-derived vascular endothelial growth factor on wound healing. *J Invest Dermatol.* 2011;131(3):797-801.
13. Qian BZ, Pollard JW. Macrophage diversity enhances tumor progression and metastasis. *Cell.* 2010;141(1):39-51.
14. Stockmann C, Doedens A, Weidemann A, et al. Deletion of vascular endothelial growth factor in myeloid cells accelerates tumorigenesis. *Nature.* 2008;456(7223):814-818.
15. Gordon S. Alternative activation of macrophages. *Nat Rev Immunol.* 2003;3(1):23-35.
16. Gordon S, Taylor PR. Monocyte and macrophage heterogeneity. *Nat Rev Immunol.* 2005;5(12):953-964.
17. Mosser DM, Edwards JP. Exploring the full spectrum of macrophage activation. *Nat Rev Immunol.* 2008;8(12):958-969.
18. Geissmann F, Jung S, Littman DR. Blood monocytes consist of two principal subsets with distinct migratory properties. *Immunity.* 2003;19(1):71-82.
19. Auffray C, Fogg D, Garfa M, et al. Monitoring of blood vessels and tissues by a population of monocytes with patrolling behavior. *Science.* 2007;317(5838):666-670.
20. Schwenk F, Baron U, Rajewsky K. A cre-transgenic mouse strain for the ubiquitous deletion of loxP-flanked gene segments including deletion in germ cells. *Nucleic Acids Res.* 1995;23(24):5080-5081.
21. Gerber HP, Hillan KJ, Ryan AM, et al. VEGF is required for growth and survival in neonatal mice. *Development.* 1999;126(6):1149-1159.
22. Hafner M, Wenk J, Nenci A, et al. Keratin 14 Cre transgenic mice authenticate keratin 14 as an oocyte-expressed protein. *Genesis.* 2004;38(4):176-181.
23. Clausen BE, Burkhardt C, Reith W, Renkawitz R, Forster I. Conditional gene targeting in macrophages and granulocytes using LysMcre mice. *Transgenic Res.* 1999;8(4):265-277.
24. Rossiter H, Barresi C, Pammer J, et al. Loss of vascular endothelial growth factor a activity in murine epidermal keratinocytes delays wound healing and inhibits tumor formation. *Cancer Res.* 2004;64(10):3508-3516.
25. Tomasek JJ, McRae J, Owens GK, Haaksma CJ. Regulation of alpha-smooth muscle actin expression in granulation tissue myofibroblasts is dependent on the intronic CArG element and the transforming growth factor-beta1 control element. *Am J Pathol.* 2005;166(5):1343-1351.
26. Gabrilovich DI, Nagaraj S. Myeloid-derived suppressor cells as regulators of the immune system. *Nat Rev Immunol.* 2009;9(3):162-174.
27. Serbina NV, Pamer EG. Monocyte emigration from bone marrow during bacterial infection requires signals mediated by chemokine receptor CCR2. *Nat Immunol.* 2006;7(3):311-317.
28. Ingersoll MA, Platt AM, Potteaux S, Randolph GJ. Monocyte trafficking in acute and chronic inflammation. *Trends Immunol.* 2011;32(10):470-477.
29. Lim JK, Obara CJ, Rivollier A, Pletnev AG, Kelsall BL, Murphy PM. Chemokine receptor Ccr2 is critical for monocyte accumulation and survival in West Nile virus encephalitis. *J Immunol.* 2011;186(1):471-478.
30. Ye M, Iwasaki H, Laiosa CV, et al. Hematopoietic stem cells expressing the myeloid lysozyme gene retain long-term, multilineage repopulation potential. *Immunity.* 2003;19(5):689-699.
31. Fukumura D, Xavier R, Sugiura T, et al. Tumor induction of VEGF promoter activity in stromal cells. *Cell.* 1998;94(6):715-725.
32. Kishimoto J, Ehama R, Ge Y, et al. In vivo detection of human vascular endothelial growth factor promoter activity in transgenic mouse skin. *Am J Pathol.* 2000;157(1):103-110.
33. Miquerol L, Gertsenstein M, Harpal K, Rossant J, Nagy A. Multiple developmental roles of VEGF suggested by a LacZ-tagged allele. *Dev Biol.* 1999;212(2):307-322.
34. De Palma M, Venneri MA, Galli R, et al. Tie2 identifies a hematopoietic lineage of proangiogenic monocytes required for tumor vessel formation and a mesenchymal population of pericyte progenitors. *Cancer Cell.* 2005;8(3):211-226.
35. Hellström M, Phng LK, Hofmann JJ, et al. Dll4 signalling through Notch1 regulates formation of tip cells during angiogenesis. *Nature.* 2007;445(7129):776-780.
36. Gerhardt H, Golding M, Fruttiger M, et al. VEGF guides angiogenic sprouting utilizing endothelial tip cell filopodia. *J Cell Biol.* 2003;161(6):1163-1177.
37. Ochoa O, Sun D, Reyes-Reyna SM, et al. Delayed angiogenesis and VEGF production in CCR2-/- mice during impaired skeletal muscle regeneration. *Am J Physiol Regul Integr Comp Physiol.* 2007;293(2):R651-R661.
38. Lu H, Huang D, Saederup N, Charo IF, Ransohoff RM, Zhou L. Macrophages recruited via CCR2 produce insulin-like growth factor-1 to repair acute skeletal muscle injury. *FASEB J.* 2011;25(1):358-369.
39. Saederup N, Cardona AE, Croft K, et al. Selective chemokine receptor usage by central nervous system myeloid cells in CCR2-red fluorescent protein knock-in mice. *PLoS One.* 2010;5(10):e13693.
40. Qian BZ, Li J, Zhang H, et al. CCL2 recruits inflammatory monocytes to facilitate breast-tumour metastasis. *Nature.* 2011;475(7355):222-225.